Field application of a novel active-passive sampling technique for the simultaneous measurement of a wide range of contaminants in water

Article Type: Research article

Field application of a novel active-passive sampling technique for the simultaneous measurement of a wide range of contaminants in water

Elvio D. Amato[a*], Fabienne Pfeiffer[b], Nicolas Estoppey[b], Dragan Subotic[c], Laure Herweyers[d], Tom Breugelmans[e], Maarten Weyn[c], Els Du Bois[d], Freddy Dardenne[a], Adrian Covaci[f], Raewyn M. Town[a] and Ronny Blust[a]

[a] Systemic Physiological and Ecotoxicological Research (SPHERE), Department of Biology, University of Antwerp, Groenenborgerlaan 171, 2020 Antwerp, Belgium

[b] School of Criminal Sciences, University of Lausanne, Batochime, 1015 Lausanne, Switzerland

[c] Internet and Data Lab (IDLab), University of Antwerp – imec, Belgium

[d] Department of Product Development, Faculty of Design Sciences, University of Antwerp, 2000 Antwerpen, Belgium

[e] Research Group Applied Electrochemistry & Catalysis (ELCAT), University of Antwerp, Universiteitsplein 1, 2610 Wilrijk, Belgium

[f] Toxicological Center, University of Antwerp, Universiteitsplein 1, 2610 Wilrijk, Belgium

* corresponding author (elvio.amato@uantwerpen.be)

Phone: +32 3265 35 33

ABSTRACT.

A first test of the field capabilities of a novel *in situ* sampling technique combining active and passive sampling (APS) was conducted in the sea. The proof-of-concept device uses a pump to draw water into a diffusion cell where dissolved target substances are accumulated onto sorbents which are selective for different classes of contaminants (i.e., metal cations, polar and non-polar organic compounds), simultaneously. A controlled laminar flow established in the diffusion cell enables measurements of contaminant concentrations that are fully independent from the hydrodynamic conditions in the bulk solution. APS measurements were consistent with those obtained using conventional passive sampling techniques such as organic diffusive gradients in thin films (o-DGT) and silicone rubber (SR) samplers (generally < 40% difference), taking into account the prevailing hydrodynamic conditions. The use of performance reference compounds (PRC) for hydrophobic contaminants provided additional information. Field measurements of metal ions in seawater showed large variability due to issues related to the device configuration. An improved field set-up deployed in supplementary freshwater mesocosm experiments provided metal speciation data that was consistent with passive sampling measurements (DGT), taking into account the hydrodynamic conditions. Overall, the results indicate that the APS technique provides a promising approach for the determination of a wide range of contaminants simultaneously, and independently from the hydrodynamic conditions in the bulk solution.

Keywords: Passive sampling; active sampling; DGT; silicone rubber; HLB; seawater

1 INTRODUCTION

Passive sampling has been increasingly used for monitoring contaminants in water, and several studies have shown its potential for applications in large scale monitoring programmes (Booij et al., 2016; Lohmann et al., 2017; Morin et al., 2012; Poulier et al., 2014). However, concerns remain on the quantitative interpretation of passive sampling measurements due to difficulties in accounting for the impact of environmental factors on the uptake of passive sampling devices (Harman et al., 2012; Morin et al., 2012; Poulier et al., 2014). Passive sampling involves the deployment of *in situ* devices which accumulate substances dissolved in aqueous media on specific sorbent materials. It is generally assumed in the passive sampling literature that when the system is far from partition equilibrium and when all physicochemical forms of the target analytes are labile on the measurement timescale (i.e., kinetics can be ignored), the accumulation of substances is rate-limited by diffusion across the diffusion layer in solution at the sorbent/medium interface, with thickness δ (Challis et al., 2016; Estoppey et al., 2014; Rusina et al., 2010). Hydrodynamic conditions in the bulk medium have a strong impact on δ, and as a consequence, also on the uptake rate of passive sampling devices (unless additional diffusion layers are used to control mass transport to the device - see further in the text). Thus, calibration is needed to estimate the effect of flow rate, as well as the effect of other environmental factors such as temperature, salinity and pH, on the uptake of passive sampling devices.

Calibration procedures usually involve the estimation of the sampling rate (R_s, $m^3\ s^{-1}$) of a given passive sampling device, and in the majority of the cases, these procedures are carried out in the laboratory (Estoppey et al., 2019; Harman et al., 2012; Morin et al., 2012); however, the lack of standardised calibration procedures often results in estimations of R_s that vary significantly for the same compound (Challis et al., 2018; Harman et al., 2012; Morin et al., 2012). In addition, unless the experimental conditions used in the calibration exercise match

69 those in the field, measurements are likely to yield to semi-quantitative results at best.
70 Calibrations performed *in situ* may offer a more adequate approach for estimating R_s (Ahrens
71 et al., 2018; Kaserzon et al., 2012; Mazzella et al., 2010), however, field calibrations are rarely
72 performed, and care should be taken to verify that environmental conditions do not
73 significantly differ from those recorded during the calibration exercise.

74 Alternative approaches exist to account for, or reduce, the impact of hydrodynamic
75 conditions on passive sampling measurements. The diffusive gradients in thin films (DGT)
76 technique relies on the use of a diffusive (hydro)gel to control the mass transport of
77 contaminants from the exposure medium to the device (Challis et al., 2018; Chen et al., 2017;
78 Davison and Zhang, 2012). The diffusive gel is placed at the interface between the sorbent and
79 the sampling medium, acting as an additional diffusion layer (of thickness Δg). The basic
80 concept of the DGT technique relies on the assumption that $\Delta g \gg \delta$, and thus, the
81 hydrodynamic conditions in the exposure medium are expected to have a negligible impact on
82 the accumulation process. While this assumption may be satisfied in many aquatic
83 environments, in some cases δ may become significant relative to Δg due to poor mixing of the
84 bulk medium, resulting in inaccurate estimations of contaminant concentrations (Challis et al.,
85 2016; Uher et al., 2013; Warnken et al., 2006).

86 Hydrophobic contaminants in water are commonly measured using sorbents such as
87 polyethylene (PE) and silicone rubber (SR) (Estoppey et al., 2016; Lohmann et al., 2017;
88 Smedes, 2019). These sorbents can be dosed with performance reference compounds (PRC),
89 which are compounds that have physico-chemical properties similar to those of target
90 substances, and that do not occur in the environment (Huckins et al., 2002). PRC-based
91 methods inherently assume that both the uptake of target substances from the bulk water and
92 the release of PRCs from the sorbent phase follow first order kinetics with the same rate
93 constants. On this basis the measured dissipation rate of PRC is used to estimate *in situ* R_s by

means of non-linear least-squares regression analysis (Booij and Smedes, 2010). PRC methods have also been used for the measurement of polar organic compounds, however, poor results were obtained due to different uptake and release kinetics observed for these compounds within the range of sorbents investigated (Buzier et al., 2019; Harman et al., 2012, 2011; Harman and Booij, 2014; Liu et al., 2013).

Recently, a novel active-passive sampling (APS) device was developed for the *in situ* determination of metal, polar and non-polar compound concentrations in water, simultaneously (Amato et al., 2019, 2018). The proof-of-concept device uses a diffusion cell loaded with three different sorbents to accumulate contaminants with varying physico-chemical properties (e.g., metals, polar and non-polar organic compounds). The diffusion cell is supplied with exposure medium by means of a pump, and a flow meter ensures accurate measurements of flow rates within the diffusion cell. A controlled laminar flow is established within the cell, enabling reliable estimations of δ. This feature allows measurements to be obtained that are fully independent from the hydrodynamic conditions in the bulk exposure medium, and overcomes limitations of conventional passive sampling approaches. In this study, the performance of the APS approach was assessed in the field through the comparison with conventional passive sampling devices, i.e., DGT, organic DGT (o-DGT), and the SR sampler. The benefits and limitations of this approach are discussed, and recommendations are provided for the future development of this technique.

2 MATERIALS AND METHODS

2.1 Chemicals and reagents

All reagents and solvents were analytical reagent grade or of equivalent analytical purity. Chelex 100 and acrylamide solution (40%) were purchased from Bio-Rad. Oasis HLB powder was obtained from Waters (USA). Silicone rubber (SR) sheets (SSP-M823, 250 µm thickness)

were purchased from Shielding-solutions (UK). Certified reference standards (CRS) of the polar target analytes (carbamazepine, diuron, isoproturon) and mass labelled analogues (carbamazepine-d2, diuron-d6, isoproturon-d6) were purchased from Sigma Aldrich. CRS of the non-polar target compounds (PCBs 28, 52, 101, 118, 138, 153 and 180, acenaphthylene (ACY), acenaphthene (ACE), fluorene (FLE), phenanthrene (PHE), anthracene (ANT), fluoranthene (FLU), pyrene (PYE), benz[a]anthracene (BaA), chrysene (CHR), benzo[a]pyrene (BaP), benzo[b]fluoranthene (BbF), benzo[k]fluoranthene (BkF), indeno[1,2,3-cd]pyrene (IDP), dibenz[a,h]anthracene (DBahA), benzo[ghi]perylene (BghiP)) were purchased from LGC Standards (Germany), their mass labelled analogues (13C-PCBs and d-PAHs) from Cambridge Isotope Laboratories (UK) and PRCs (biphenyl-d10, PCBs 1, 2, 3, 10, 14, 21, 30, 50, 55, 78, 104, 145, and 204) from Dr. Ehrenstorfer (Germany).

2.2 Active-passive sampling device

The APS device consists of a polyether ether ketone (PEEK) diffusion cell (Figure S1 of the Supporting Information (SI)) which features a pump on the inlet, and a flow meter on the outlet (Amato et al., 2019). A two-layer stainless steel filter, containing a mesh of 400 µm followed by a mesh of 120 µm, was connected to the pump to prevent coarse material from entering the diffusion cell. During exposure to seawater, biofouling forming on filters was removed weekly. The diffusion cell is comprised of two blocks separated by a 5 mm thick spacer. One block contains two pockets to accommodate a polyacrylamide Chelex binding gel (compartment A1) and an agarose HLB binding gel (compartment A2), respectively, whilst the second block contains a pocket designed to host a SR strip (compartment B) (Figure S1). Chelex and HLB binding gels were topped with a 800 µm thick polyacrylamide and a 750 µm thick agarose diffusive gel, respectively. Finally, the polyacrylamide diffusive gel was topped with a filter membrane (polyethersulfone (PES), 0.45 µm pore size, 100 µm thickness). The procedures

144 used for the preparation, handling and extraction of gels and SR strips are analogous to those
145 used for conventional passive sampling techniques and are described in the SI.
146
147 *2.3 Field study*
148 Field experiments were conducted in the Port of Zeebrugge, on the Belgian coastline of the
149 North Sea. Sampling devices were hung from a floating pontoon at a depth of 0.3 m (Figure
150 S2). DGT and o-DGT devices were loaded on plastic and aluminium holders, respectively,
151 fixed onto the pontoon using plastic ropes. SR sheets were attached to stainless steel bars that
152 were fixed to the pontoon by means of metal chains. APS devices were fixed on the pontoon
153 by means of metal chains, with the diffusion cell held a few centimetres above the water level,
154 and the filter submerged a few centimetres below the water level. For all sampling devices,
155 measurements were performed in triplicate. Details on the preparation and handling of DGT,
156 o-DGT and SR devices are provided in the SI. Sampling devices specifications are reported in
157 Table S1.
158 APS and passive sampling devices were deployed simultaneously and a range of
159 deployment times were implemented: the HLB sorbent for polar organic compounds was left
160 *in situ* for periods of 6, 8, and 15 days (an additional 3.5 day deployment was performed for
161 the APS device); the SR sorbent for non-polar organic compounds was left for 6 and 30 days;
162 and the Chelex sorbent for metal cations was left *in situ* for 8 and 15 days.
163 Discrete water samples (DWS) were periodically collected for the determination of
164 metal and polar organic compounds concentrations, filtered (PES, 0.45 µm) and stored at 4 °C.
165 Polar organic compound concentrations were determined by liquid-liquid extraction following
166 procedures adapted from previous work (Amato et al., 2018); to improve detection, the volume
167 of sample was increased from 5 to 25 mL. Physicochemical parameters of the exposure
168 medium (pH, conductivity, temperature and oxygen) were monitored throughout each

exposure period (Table S2). Details on the analytical methods used for sample preparation and analysis are provided in the SI.

2.4 QA/QC

For each sampling event, one set of passive sampling devices was deployed in water in triplicate, and another set was exposed to the air during installation and retrieval operations and used as field blanks. For the APS device, blanks consisted of unexposed sorbents. Additional information is provided in the SI.

2.5 Data analysis

Concentrations measured by the DGT, o-DGT, and APS device were estimated assuming a steady-state limiting diffusive flux (here-on simply referred to as steady-state diffusive flux) for the entire duration of the exposure (i.e., at the water/sorbent interface the concentration of the target species in the aqueous medium is zero, there is negligible contribution from the initial transient, and uptake conditions remain far from partition equilibrium). The time-averaged flux measured by the DGT and APS devices can be used to estimate the concentration of free and labile species (mmol dm^{-3}) in the bulk medium according to:

$$C_{\mathrm{DGT/APS}} = \frac{N(\Delta g+\delta)}{DAt} \qquad [\mathrm{mmol\ dm^{-3}}] \qquad (1)$$

where N (mol) is the moles of substance accumulated on the receiving sorbent phase, δ the thickness of the aqueous diffusion layer at the device/medium interface (m), Δg is the combined thickness of the diffusive gel and filter membrane (when included) (m), D the diffusion coefficient ($m^2\ s^{-1}$) of a given contaminant in the exposure media at a given temperature, A (m^2) the sampling area of the device, and t (s) the duration of the exposure (Davison and Zhang, 2012). Diffusion coefficients of metal ions in water and polyacrylamide diffusive gels were obtained from Li and Gregory (1974) and Scally et al. (2006), respectively; diffusion

coefficients for organic compounds measured in agarose hydrogels (1.5 % m/v agarose) were obtained from our previous work (Amato et al., 2018), and used as an approximation of diffusion coefficients in water. All diffusion coefficients were temperature-corrected (Amato et al., 2018). For DGT measurements of metal cations, δ was assumed to be 200 µm (Gaulier et al., 2019), whereas for o-DGT measurements of polar organic compound measurements, δ was estimated experimentally (see further in the text). The average thickness of the aqueous diffusion layer $\bar{\delta}$ at the interface of the sorbents loaded in the APS diffusion cell was estimated using

$$\bar{\delta} = 1.4327\, D^{1/3}\, d^{1/3}\, h^{2/3}\, L^{1/3} \left(\frac{1}{V_f}\right)^{1/3} \quad \text{[m]} \qquad (2)$$

where d, h and L are geometric parameters that refer to ½ the width, ½ height, and the length of the exposed area of the sorbent (m), respectively, and v_f is the flow rate ($m^3\ s^{-1}$) within the diffusion cell (Amato et al., 2019; Tomaszewski et al., 2003). In this study, the average flow rate within the diffusion cell ranged between 7.1 and 7.5 mL s^{-1} (equivalent to a flow velocity of 7.1-7.5 cm s^{-1}, estimated by dividing the flow rate by the cross-sectional area of the exposure chamber within the diffusion cell; Figure S1), and estimated $\bar{\delta}$ ranged between 71 and 90 µm, 85 and 98 µm, and 73 and 80 µm, for metals, polar and non-polar organic compounds, respectively.

Non-polar organic compound concentrations measured using the SR sampler were estimated following a method described by Smedes and Booij (2012). According to this method, the fraction of PRC (f) retained in the SR sheet is described by

$$f = \frac{N_t}{N_0} = \exp\left(-\frac{B\,t}{K_{pw}\, MW^{0.47}\, m}\right) \qquad (3)$$

where N_t is the amount of PRC found at the end of the exposure (mol), N_0 is the dosed amount measured in the reference SR sheets (mol), B is an empirical constant that depends on the temperature and hydrodynamic conditions in the bulk medium and is proportional to the

exposed surface area of the sorbent ($g^{0.47}$ m^3 $mol^{-0.47}$ s^{-1}), K_{pw} is the polymer-water partition coefficient (m^3 kg^{-1}) (Smedes, 2019), adjusted to salinity according to Jonker and Muijs (2010), and m is the mass of polymer sheet (kg). The parameter B is estimated by plotting f against K_{pw} $MW^{0.47}$ and by fitting data using non- linear least- squares analysis (Booij and Smedes, 2010). Once B is estimated, concentrations (C_{SR}) in the bulk medium can be calculated using

$$C_{SR} = \frac{N_t}{K_{pw} m \left(1 - \exp\left(-\frac{B\,t}{K_{pw}\,MW^{0.47} m}\right)\right)} \quad \text{[mmol dm}^{-3}\text{]} \quad (4)$$

PRC were spiked also on SR strips loaded on the APS device, and thus, C_{APS} could be calculated using both Eq.1 and Eq. 4. First-order kinetics were assumed for the estimation of the half-time to equilibrium partition ($\tau_{1/2}$) according to

$$\tau_{1/2} = \frac{\ln(2) K_{pw} m MW^{0.47}}{B} = \frac{\ln(2) K_{pw} m \delta}{AD} \quad \text{[s]} \quad (5)$$

All average values are reported with standard error (SE).

3 RESULTS AND DISCUSSION

3.1 Polar organic compounds

Concentrations of carbamazepine measured using the APS and o-DGT devices were in good agreement (<15% difference) following deployments of 6 days and 8 days (Table 1). After 15 days exposure, extensive damage and loss of diffusive gels (and in some cases also of HLB binding gels) were observed for both APS and o-DGT devices. In contrast, no damage was observed after 4 (performed only for the APS device), 6 and 8 days exposures, suggesting that the loss of diffusive/binding gels was linked to the duration of the exposure to seawater. Previous o-DGT measurements performed in a similar location and using analogous agarose gels (i.e., 1.5% (w/v) agarose) did not show damage or loss of gels after an exposure of 14 days likely because the devices included a protective filter membrane placed on top of the diffusive gel (Guo et al., 2019). A previous study also reported damage to the agarose diffusive gel,

242 which was attribute to grazing of aquatic insects (Challis et al., 2018). However, it may be
243 useful to investigate alternative gel materials such as polyacrylamide, which have been seldom
244 used for measurements of polar organic compounds (Stroski et al., 2018).
245
246 **Table 1.** Dissolved organic compound concentrations measured using the APS, o-DGT and
247 discrete water samples (DWS) (mean ± SE). All measurements were performed in triplicates,
248 except for DWS (n = 4 or 5). All concentrations are reported in pmol dm^{-3}.

	6 days			8 days		
Substance	APS	o-DGT	DWS	APS	o-DGT	DWS
Carbamazepine	52.8 ± 1.3	60.3 ± 1.0	39.5 ± 2.4	74.4 ± 6.1	80.8 ± 7.3	52.0 ± 5.8
Diuron	<3	<16	<15	13.7 ± 1.5	13.5 ± 1.2	<15
Isoproturon	<2	<8	<7	1.34 ± 0.15	<3	<7

	6 days			30 days		
Substance	APS-SS	APS-PRC	SR	APS-SS	APS-PRC	SR
ACY	4.11 ± 0.09	10.4 ± 0.1	12.4 ± 0.3	0.555 ± 0.059	8.16 ± 0.69	5.95 ± 0.22
ACE	112 ± 3	148 ± 2	183 ± 7	16.1 ± 1.6	90.7 ± 7.7	59.6 ± 0.8
FLE	32.2 ± 1.4	38.4 ± 0.6	50.8 ± 2.2	4.87 ± 0.39	20.6 ± 1.3	15.2 ± 0.2
PHE	37.3 ± 3.3	38.4 ± 1.3	48.3 ± 0.3	6.91 ± 0.22	16.9 ± 0.3	12.2 ± 0.4
ANT	11.4 ± 1.7	11.2 ± 1.2	10.9 ± 0.4	1.95 ± 0.09	4.01 ± 0.20	2.83 ± 0.07
FLU	47.0 ± 2.6	44.7 ± 1.1	61.7 ± 2.4	28.1 ± 0.2	32.4 ± 0.5	32.1 ± 0.5
PYE	30.3 ± 1.9	28.3 ± 0.1	36.5 ± 1.0	15.9 ± 0.2	16.5 ± 0.3	12.4 ± 0.5
BaA	2.53 ± 0.15	2.42 ± 0.07	3.67 ± 0.13	1.58 ± 0.05	1.31 ± 0.01	1.25 ± 0.06
CHR	4.38 ± 0.08	4.20 ± 0.22	6.25 ± 0.56	3.29 ± 0.10	2.74 ± 0.09	3.16 ± 0.05
BbF	1.09 ± 0.02	1.08 ± 0.07	1.83 ± 0.11	1.01 ± 0.03	0.798 ± 0.010	0.874 ± 0.040
BkF	<0.45	<0.45	0.537 ± 0.063	0.333 ± 0.015	0.264 ± 0.004	0.362 ± 0.017
BaP	<0.45	<0.45	0.367 ± 0.017	0.156 ± 0.006	0.125 ± 0.002	0.109 ± 0.007
IDP	<1.20	<1.20	0.291 ± 0.046	<0.20	<0.20	0.071 ± 0.003
DBahA	<1.20	<1.20	<0.124	<0.20	<0.20	0.022 ± 0.001
BghiP	<1.06	<1.06	0.380 ± 0.070	<0.18	<0.18	0.062 ± 0.005
CB28	<0.25	<0.25	0.047 ± 0.002	0.047 ± 0.000	0.038 ± 0.001	0.035 ± 0.001
CB52	<0.14	<0.14	0.050 ± 0.003	0.046 ± 0.001	0.038 ± 0.001	0.034 ± 0.001
CB101	<0.13	<0.13	0.033 ± 0.001	0.028 ± 0.001	0.024 ± 0.001	0.019 ± 0.000
CB118	<0.41	<0.41	<0.026	<0.07	<0.07	0.009 ± 0.000
CB153	<0.36	<0.36	0.037 ± 0.001	<0.06	<0.06	0.019 ± 0.001
CB138	<0.22	<0.22	0.018 ± 0.001	<0.04	<0.04	0.007 ± 0.000
CB180	<0.38	<0.38	<0.026	<0.06	<0.06	<0.005

249

The uptake of the APS device was linear up to 8 days (Figure S3), and, given the identical diffusive gel and the similar amount of sorbent used (i.e., Δg = 750 µm), linear uptake was assumed also for the o-DGT device. This assumption can be made if $\Delta g \gg \delta$. For the APS device, δ was calculated using Eq. 2 (~90 µm). For the o-DGT device, δ was calculated using a method which involves the simultaneous deployment of devices with varying Δg (e.g., 250, 500 and 750 µm). According to this method, the reciprocal of the accumulated mass measured after exposure is plotted against Δg, and the x-intercept of the obtained regression curve gives an estimate of δ (Figure S3) (Challis et al., 2018; Chen et al., 2013). The regression analysis provided a δ of 130 µm, which is in the range of δ observed for polar organic compounds under similar hydrodynamic conditions (Challis et al., 2018; Chen et al., 2013; Guo et al., 2019), and was about 6 times smaller than the Δg commonly used for standard o-DGT deployments (i.e., 750 µm).

While carbamazepine concentrations in seawater measured using the APS and the o-DGT devices were overall in good agreement, they were consistently greater than concentrations measured in DWS (~30 and ~50% for APS and o-DGT, respectively) (Table 1). Since DWS concentrations represent a measure of all dissolved chemical species of a substance present in the aqueous phase (i.e., the total dissolved fraction), C_{APS} and $C_{o\text{-}DGT}$ are expected to be $\leq C_{DWS}$. Overestimation of dissolved concentrations may also be linked to the degradation of the agarose diffusive gel, which may have led to a decrease in Δg, and thus an increase in the accumulation rate (Eq. 1).

Isoproturon concentrations were between LOD and LOQ of the respective methods, except for APS measurements performed for 8 days (Table 1; Table S3). This was due to the larger exposed surface area of the APS sorbent compared to that of the o-DGT (8.0×10^{-4} and 3.14×10^{-4} m^2, respectively; Table S1). Similarly, diuron concentrations were consistently between LOD and LOQ, except for APS and o-DGT exposures of 8 days, which were in strong

agreement with each other (Table 1; Table S3). These results overall indicated that the APS device allows reliable measurements of polar organic compounds. In addition, by removing the diffusion gel placed on top of the HLB gel, the uptake rate of the APS will increase, thereby allowing lower detection limits to be achieved while maintaining controlled flow conditions (Amato et al., 2019).[25]

3.2 Non-polar organic compounds

3.2.1 PCBs

APS measurements of both PCBs and PAHs were interpreted using two approaches: (i) by assuming a steady-state diffusive flux throughout the entire duration of the exposure (Eq. 1), and (ii) by using dissipation rates of PRC from dosed SR sorbents (Eq. 4). After 30 days exposure, all target PCB were detected by both the APS and SR devices, however, CB-118, -138, -153, and -180 were below the LOQ of the APS device (Figure 1A; Table 1; Table S3). This was due to the considerably smaller exposed surface area of the sorbent used in the APS device compared to that used by the SR device (2.0×10^{-3} and 7.2×10^{-2} m^2 respectively; Table S1). For the compounds that exceeded the LOQ, APS-PCB concentrations estimated assuming a steady-state diffusive flux ($C_{APS\text{-}SS}$) were in strong agreement with, but consistently greater (~20%) than concentrations estimated using the PRC approach ($C_{APS\text{-}PRC}$) (Figure 1A; Table 1). The PRC method allows to estimate concentrations in water irrespective of whether the system is far from, has attained, or is approaching equilibrium (Booij and Smedes, 2010). Thus, the agreement observed between $C_{APS\text{-}SS}$ and $C_{APS\text{-}PRC}$ indicates that a steady-state diffusive flux existed for essentially the entire duration of the deployment, validating the use of Eq. 1 to estimate PCB concentrations under the experimental conditions used. This was also in agreement with estimations of the linear uptake range obtained based on K_{pw} (Eq. 5), which indicated that the deployment time was $\ll \tau_{1/2}$ (Table S4). APS measurements were also in

satisfactory agreement with those obtained using the SR device, i.e., $C_{APS\text{-}SS}/C_{SR}$ ratios were between 1.3 and 1.5, and $C_{APS\text{-}PRC}/C_{SR}$ were between 1.1 and 1.3, respectively (for C_{APS} > LOQ) (Figure 1).

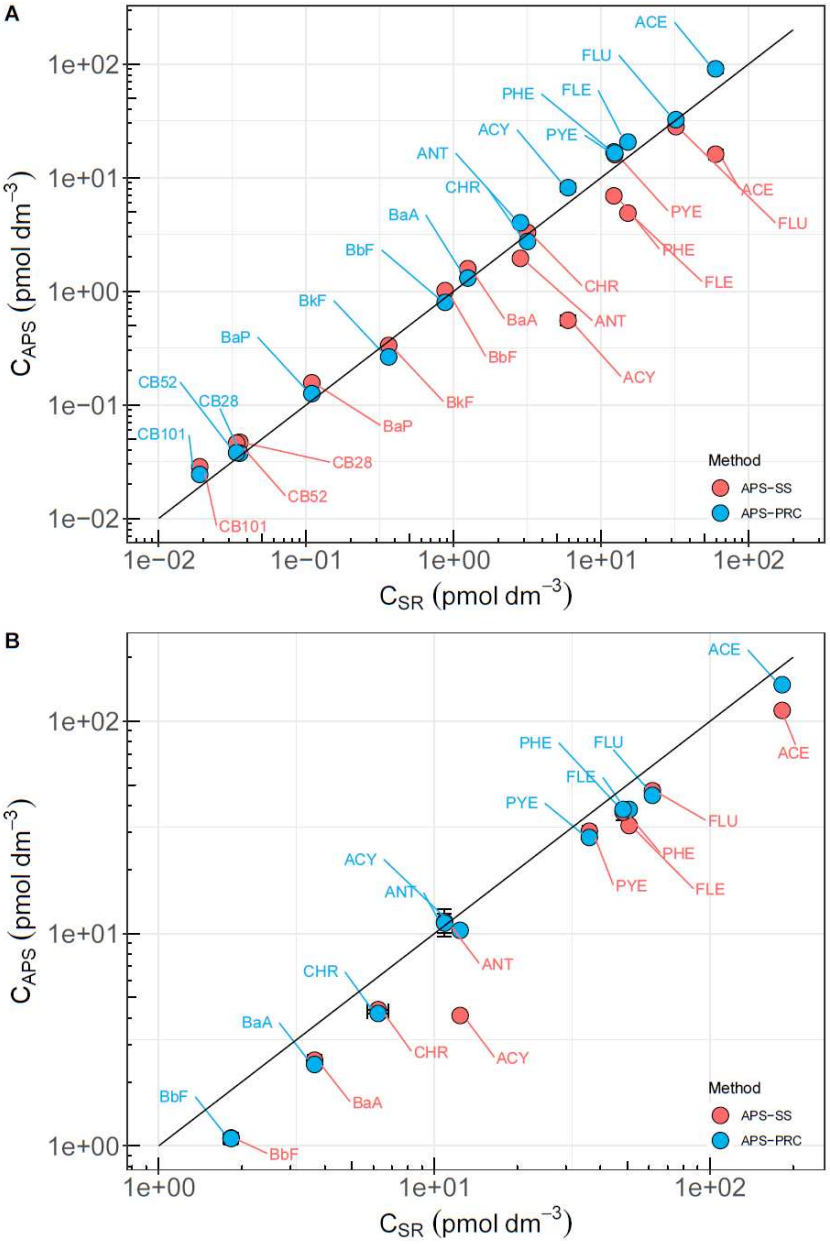

Figure 1. Comparison between PAH and PCB concentrations in the bulk aqueous medium measured using the APS (C_{APS}) and SR (C_{SR}) devices (mean ± SE). Panels (A) and (B) refer to deployments of 30 and 6 days, respectively. APS concentrations were calculated assuming a

steady-state diffusive flux for the entire duration of the exposure (red circles), and using the retained fraction of PRC (blue circles). The solid line represents a 1:1 relationship.

After 6 days exposure, concentrations of all PCB congeners were below the LOQ (and often also the LOD) of the APS device (Table 1; Table S3). This was due to the very low concentration levels in the water body and the relatively short exposure time, which contributed to the small amount of PCB accumulated on the device. In contrast, due to its considerably larger exposed surface area, CB-28, -52, -101, -138 and -153 concentrations could be quantitatively measured by the SR device (1.5 ~ 5.0 $\times 10^{-2}$ pmol dm^{-3}).

3.2.2 PAHs

All PAHs were detected after APS and SR deployments of 30 days, although some compounds were < LOQ of the APS device (i.e., IDP, DBahA, BghiP) (Table 1; Table S3). For concentrations that exceeded the LOQ, $C_{APS\text{-}SS}$ were in strong agreement with $C_{APS\text{-}PRC}$ (< 30% difference) for compounds that were expected to be far from equilibrium (i.e., $t < \tau_{1/2}$, FLU, PYE, BaA, CHR, BbF, BkF, BaP; Figure 1A, Table S4), whilst $C_{APS\text{-}SS} \ll C_{APS\text{-}PRC}$ for compounds predicted to have attained equilibrium (i.e., $t > \tau$ for ACY, ACE, FLE, PHE, ANT; Figure 1A; Table S5). This was expected because $C_{APS\text{-}SS}$ is calculated based on the assumption of steady-state diffusive flux (Eq. 1), which was incorrect for these compounds under the experimental conditions used. A similar trend was observed when comparing APS-SS to SR measurements, with $C_{APS\text{-}SS}$ differing from C_{SR} of < 30% for compounds predicted to follow steady-state uptake kinetics (except for BaP, 43% difference), and $C_{APS\text{-}SS}$ < or $\ll C_{SR}$ for compounds predicted to have attained equilibrium (Figure 1A, Table S5). In contrast, $C_{APS\text{-}PRC}$ were in good agreement with C_{SR} irrespective of whether compounds attained equilibrium or

not (< 40% difference, except for ACE) (Figure 1A). This is due to the term $1 - \exp\left(-\frac{B\,t}{K_{pw}\,MW^{0.47}m}\right)$ $\rightarrow 1$ for $t \rightarrow \infty$, which reduces Eq. 4 to

$$C_{SR} = C_{eq} = \frac{N_t}{K_{pw}m} \quad \text{(mmol dm}^{-3}\text{)} \quad \text{Eq. 6}$$

where C_{eq} corresponds to the equilibrium concentration of the sorbent-partitioning form(s) of the substance in the bulk aqueous medium. $C_{APS\text{-}PRC}$ closely approached C_{eq} for compounds that were expected to have attained equilibrium (i.e., $C_{APS\text{-}PRC}/\ C_{eq}$ = 1.03, 1.03, 1.03, 1.06 and 1.09 for ACY, ACE, FLE, PHE, and ANT, respectively), consistent with the theory described above. A similar trend was observed for C_{SR}, although C_{SR} appeared to slightly underestimate C_{eq} (i.e., $C_{SR}/\ C_{eq}$ = 0.75, 0.59, 0.76, 0.75 and 0.77 for ACY, ACE, FLE, PHE and ANT, respectively).

Measurements performed over a 6 days exposure showed trends similar to those observed for the 30 day exposure (Figure 1; Table 1). PAH concentrations were generally above the LOQ of the APS device, except for BaP, IDP, DBahA and BghiP, whilst for the SR device, all compounds could be quantified. Overall, $C_{APS\text{-}SS}$ were in strong agreement with $C_{APS\text{-}PRC}$ (< 16% difference) except for ACY, which was predicted to have approached equilibrium (Figure 1B, Table S5). This was confirmed by the strong agreement between $C_{APS\text{-}PRC}$ (10.3 ± 0.1 pmol dm^{-3}) and C_{eq} (9.7 ± 0.1 pmol dm^{-3}). ACE and PHE were predicted to be in the semi-linear uptake phase towards the end of the exposure (i.e., $\tau_{1/2} < t < \tau$; Table S4; Table S5), however, the good agreement between $C_{APS\text{-}SS}$ and $C_{APS\text{-}PRC}$ suggests that a steady-state uptake was predominant. In general, APS and SR measurements were also in good agreement, with C_{APS} within 40% of C_{SR} for compounds found at concentrations > LOQ (Figure 1B; Table S3), except for ACY, which was predicted to have attained equilibrium (Table S5).

3.3 Metals

APS metal concentrations were consistently lower than those measured using the DGT device, except for lead and zinc, for the 8 day exposure, and nickel, for the 15 day exposure, respectively (Figure 2A; Table 2). Greater APS concentrations could be due to corrosion of some parts of the stainless steel filters placed at the inlet of the APS device, which may have caused leaching of metal ions resulting in greater diffusive fluxes towards the Chelex binding gel.

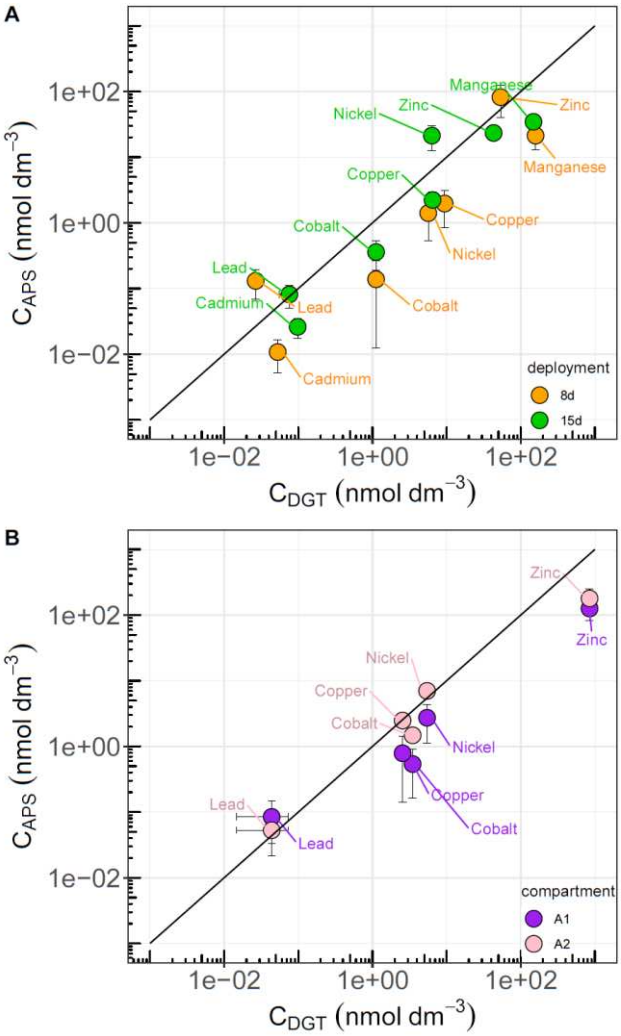

Figure 2. Comparison between metal ion concentrations in the bulk aqueous medium derived from APS and DGT measurements (A) after 8 and 15 days exposure, and (B) with Chelex binding gels loaded in compartments A1 and A2 of the APS device (7 days exposure) (mean ± SE). The solid lines represent 1:1 relationships.

Table 2. Dissolved metal concentrations measured using the APS, DGT, and discrete water samples (DWS) (mean ± SE). All measurements were performed in triplicates, except for APS measurements of 4 hours (n = 2) and DWS (n = 4 or 5). NA = not available. All concentrations are reported in nmol dm^{-3}.

	Seawater - 8 days			Seawater - 15 days			Seawater - 7 days			Laboratory - 4 hours			Freshwater Mesocosm - 4 days		
Substance	APS	DGT	DWS	APS	DGT	DWS	APS - A1	APS - A2	DGT	APS - A1	APS - A2	DWS	APS	DGT	DWS
Cd	<0.03	0.05 ± 0.00	<0.22	0.03 ± 0.01	0.10 ± 0.00	<0.22	<0.03	<0.02	<0.03	663	707	753 ± 12	4.92 ± 0.12	5.53 ± 0.06	6.86 ± 0.08
Co	0.14 ± 0.13	1.12 ± 0.06	<0.42	0.36 ± 0.17	1.12 ± 0.03	<0.42	0.54 ± 0.38	1.48 ± 0.09	3.48 ± 0.32	1385	1485	1550 ± 16	8.95 ± 0.33	10.8 ± 0.1	16.9 ± 0.3
Cu	1.97 ± 1.11	9.41 ± 0.17	30.2 ± 2.3	2.23 ± 0.75	6.47 ± 0.40	19.3 ± 2.7	0.79 ± 0.64	2.48 ± 0.08	2.55 ± 0.19	259	257	323 ± 2	4.11 ± 0.19	8.88 ± 0.27	50.2 ± 1.9
Mn	21.3 ± 8.2	158 ± 6	183 ± 36	34.6 ± 10.5	148 ± 6	187 ± 26	na	na	na	1543	1675	1710 ± 14	13.70 ± 0.41	18.8 ± 0.2	30.4 ± 1.4
Ni	1.41 ± 0.87	5.66 ± 0.11	<0.43	21.3 ± 8.8	6.33 ± 0.20	<0.43	2.73 ± 1.62	7.01 ± 0.36	5.45 ± 0.01	1297	1390	1457 ± 16	8.85 ± 0.27	15.9 ± 0.2	36.6 ± 0.7
Pb	0.13 ± 0.06	0.03 ± 0.00	<0.12	0.08 ± 0.03	0.08 ± 0.02	<0.12	0.08 ± 0.06	0.05 ± 0.02	0.04 ± 0.03	71	70	87 ± 3	0.55 ± 0.01	0.59 ± 0.00	5.28 ± 0.02
Zn	82.1 ± 42.2	53.4 ± 0.9	101 ± 26	23.4 ± 5.2	43.0 ± 2.8	100 ± 25	126 ± 43	179 ± 70	847 ± 99	930	1023	1040 ± 7	123 ± 6	118 ± 2	194 ± 4

372 The difference between APS and DGT measurements varied largely among metals, ranging
373 between ~10% and ~500%. The reproducibility of APS measurements was surprisingly poor
374 and inconsistent with previous laboratory studies (Amato et al., 2019, 2018), i.e., SE% varied
375 from 39 to 91%, and from 22 to 47%, for deployments of 8 and 15 days, respectively (n = 3).
376 In contrast, SE% for DGT measurements were < 9% (except for Pb for the 15 day deployment,
377 SE% = 27%; n = 2 and 3 for 8 day and 15 day measurements, respectively), and overall in good
378 agreement with results from previous measurements performed in this location (Gaulier et al.,
379 2019). Dissolved metal concentrations in DWS were generally below the LOQ of the method,
380 except for copper, manganese, and zinc (Table 2). DGT-Cu concentrations were 31 and 34%
381 of dissolved concentrations for 8 and 15 day deployments, respectively. This was in agreement
382 with previous speciation analysis performed in this location (Gaulier et al., 2019), and
383 consistent with the reduced lability of copper due to the presence of relatively strongly
384 complexing organic ligands (Macoustra et al., 2019; Strivens et al., 2020). DGT-Mn and -Zn
385 concentrations were 13~19%, and 47~57% lower than dissolved zinc concentrations measured
386 in DWS, respectively.

387 To investigate potential issues related to the position of the sorbent within the diffusion
388 cell, additional APS measurements were performed by loading Chelex binding gels in
389 compartment A1 as well as A2, and compared to parallel DGT deployments. As previously
390 observed, concentrations measured using compartment A1 were consistently lower than those
391 measured by DGT, and displayed the same large variability (Figure 2B; Table 2). In contrast,
392 measurements performed using compartment A2 were considerably more reproducible for all
393 metals, and the level of agreement between APS and DGT concentrations significantly
394 improved for lead, copper and nickel, with C_{APS}/C_{DGT} ratios of 1.21, 0.97, and 1.29,
395 respectively (Figure 2B; Table 2). This suggested that the field set-up did not allow for accurate
396 measurements using compartment A1; it is unclear how field conditions may have affected the

397 measurement in this specific compartment of the diffusion cell, however, the intense tidal
398 movement in the field may have contributed to the formation of air pockets in the proximity of
399 compartment A1. Also cobalt measurements were more consistent between the two techniques,
400 with a C_{APS}/C_{DGT} ratio of 0.42. Different results were obtained for zinc measurements, i.e.,
401 APS concentrations were 5-fold lower than those measured by the DGT technique. C_{APS}/C_{DWS}
402 and C_{DGT}/C_{DWS} ratios for zinc were 0.53 and 2.49, respectively. C_{APS}/C_{DWS} ratios were in
403 agreement with C_{DGT}/C_{DWS} ratios obtained for the 8 and 15 days exposures (0.53 and 0.43,
404 respectively), suggesting that DGT-Zn measurements in this last comparative test may have
405 not been reliable (i.e., C_{APS}/C_{DWS} = 2.49). However, DWS largely varied during the 7-day
406 exposure, and may have not adequately represented the real time-averaged concentrations.
407 Since the set-up used in the field appeared to yield inconsistent APS metal
408 measurements, additional tests were carried out using a custom-made casing consisting of a
409 floating device designed to host the diffusion cell, pump, and flowmeter (Figure S4). First, the
410 APS device was exposed to artificial freshwater (Table S2) for 4 hours under laboratory
411 conditions, and after, directly deployed in an artificial freshwater pond (3500 L) (Table S2) for
412 4 days. One day prior to the test commencement, the exposure media were spiked with a
413 mixture of metals and allowed to equilibrate under gentle stirring. For both tests, diffusive gels
414 were not included in the APS diffusion cell to allow for a more accurate evaluation of the effect
415 of the new set-up on the metal accumulation rate. The results of the laboratory experiment
416 indicated a strong agreement between APS metal concentrations and average dissolved metal
417 concentrations measured using DWS (<20% difference), irrespective of whether the Chelex
418 gel was placed in compartment A1 or A2 (Figure 3A; Table 2). The average accuracies (i.e.,
419 $C_{APS}/C_{DWS}\times100$) were 87 and 92% for measurements performed using compartment A1 and
420 A2, respectively. Since metal measurements performed using this new set-up were satisfactory,
421 the following tests were carried out by loading the Chelex gel in A1 only.

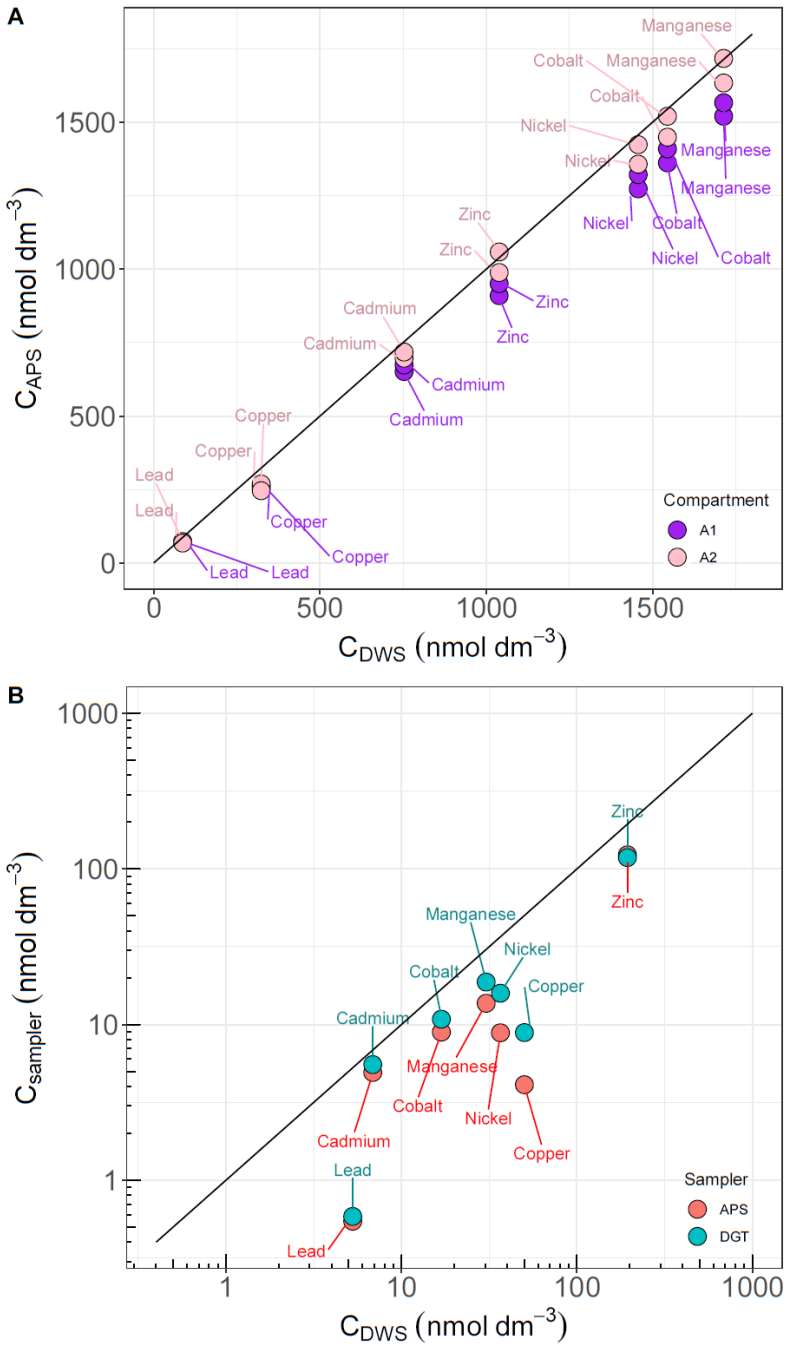

422

423 **Figure 3.** (A) Comparison between APS (n = 2) and DWS (mean ± SE, n = 4) metal ion
424 concentrations measured in the laboratory test (4 hours exposure); (B) comparison between
425 APS, DGT and DWS metal ion concentrations (mean ± SE, n = 3, 3, and 5, respectively)
426 measured in the mesocosm test (4 days exposure). Error bars that are smaller than data points
427 do not appear on graphs. The solid lines represent 1:1 relationships.

Metal concentrations measured in the freshwater mesocosm followed the general trend $C_{APS} \leq C_{DGT} < C_{DWS}$ (Figure 3B; Table 2). This was probably due to the presence of relatively high concentrations of DOC (4.54 mg dm^{-3}), which likely formed metal complexes that have a lower mean diffusion coefficient than that for the free metal ion and/or are partially labile (kinetically controlled contribution) or inert on the DGT timescale ($[\Delta g^2/(2D)] \approx 900$ s), and, even more so, on the APS timescale ($[\Delta g^2/(2D)] \approx 5$ s). Overall, in the mesocosm experiment APS concentrations were consistent with DGT concentrations (<27% difference), except for nickel (44% difference) and copper (54% difference). These results indicate that, with the upgraded APS device, reliable field measurements may be achieved also for metals. For both laboratory and mesocosm tests, the moles of metal accumulated on the APS device were from 8 to 16 times greater than those accumulated on the DGT. This indicates that, for a given exposure time, the APS device can achieve much lower detection limits compared to the DGT device (provided that the sorbent is far from approaching equilibrium).

3.4 Considerations on the use of the APS device

The conditions necessary to interpret APS measurements as time-averaged concentrations (i.e., steady-state uptake flux) were verified for deployments of 8 and 30 days for polar organic compounds and PCB, respectively, while for PAHs, the linear uptake range varied based on the compound (and relative K_{ow}). However, longer measurements of polar organic compounds that still fall within the linear uptake range are likely to be feasible (Challis et al., 2018; Guo et al., 2019). Comparisons between APS concentrations measured assuming steady-state diffusive flux conditions and using PRCs indicated that, under the experimental conditions used, a simple and reliable approximation of the integrative window can be obtained using Eq. 5. This allows to evaluate whether APS measurements can be interpreted as time-averaged concentrations or equilibrium concentrations. Results indicated that (i) for $t < \tau_{1/2}$, C_{APS}-

453 $_{SS}/C_{APS\text{-}PRC}$ = 1.02 ± 0.07 (n = 19); (ii) for $\tau_{1/2} < t < \tau$, $C_{APS\text{-}SS}/C_{APS\text{-}PRC}$ = 0.86 ± 0.10 (n = 3);
454 (iii) for $t > \tau$, $C_{APS\text{-}SS} = C_{APS\text{-}PRC} = C_{eq}$ (based on measurements for which concentrations >
455 LOQ). In principle, the same approach could be applied to polar organic compounds. These
456 results indicate that the APS approach overcomes the need to use PRCs, and also diffusive gels
457 (Amato et al., 2019).
458
459 **4 CONCLUSIONS**
460 The APS technique provides a relatively simple and effective method for the reliable
461 interpretation of contaminant concentrations in water irrespective of the hydrodynamic
462 conditions in the bulk exposure medium. Longer exposure times are required to match LOQ of
463 passive sampling devices for monitoring of hydrophobic compounds, however, APS
464 deployments of 30 days are adequate for compliance with water quality guidelines. In addition,
465 increased accumulation and lower LOQ can be achieved by increasing the flow within the cell
466 (i.e., by reducing $\bar{\delta}$) and/or the exposed surface area (obtained upon modification of the
467 diffusion cell). Overall, after accounting for the hydrodynamic conditions, the performance of
468 the APS and passive sampling devices were similar, indicating that the APS approach is useful
469 for monitoring a wide range of contaminants simultaneously. In seawater deployments,
470 diffusive gels were used to allow a direct comparison with DGT and o-DGT measurements,
471 however, by excluding diffusion gels from the APS device, the uptake of metals and polar
472 organic compounds will dramatically increase, providing much lower LOQ (as shown in the
473 freshwater mesocosm and laboratory experiments). In addition, when polyacrylamide diffusive
474 gels are used, the interpretation of DGT data requires further considerations for measurements
475 that are made (i) at low ionic strengths typical of freshwaters, where a Donnan potential
476 difference is established between the gel phase and the bulk aqueous medium (Yezek and van
477 Leeuwen, 2005; Yezek et al., 2008), and (ii) in the presence of humic substances which

accumulate in the gel phase (van der Veeken et al., 2010; van der Veeken and van Leeuwen, 2010; van Leeuwen, 2016). In seawater, agarose gels may suffer damage, as observed in this study. Furthermore, DGT measurements performed under relatively low flow conditions may result in increased uncertainty and require additional measurements for estimating δ (Chen et al., 2017). Metal measurements performed in freshwater complexing media (i.e., mesocosm experiment) suggested that the APS device can be useful for dynamic speciation analyses of contaminants in water due to its ability to manipulate δ by controlling the flow within the diffusion cell (Amato et al., 2019). This offers the possibility to make speciation measurements over a range of timescales, thereby generating a kinetic spectrum of data that can be interpolated to address questions of bioavailability (van Leeuwen et al., 2005). This feature has important implications for environmental risk assessment and merits further investigation.

■ ACKNOWLEDGMENTS

This work was conducted within the framework of the EnviroStress and Exposome Centers of Excellence at the University of Antwerp and with financial support from the Research Foundation – Flanders (FWO) (grant numbers 12V5519N and G051117N). Authors greatly acknowledge Thierry François and the Naval Base Zeebrugge, Belgium, for support during sampling operations.

Supporting Information

Analytical methods; Limits of quantification; Preparation and handling of passive sampling devices and sorbents; additional QA/QC; Figure S1. Schematic drawing of the APS diffusion cell; **Figure S2.** Picture of the field set-up; **Figure S3.** Moles of carbamazepine accumulated on the APS device as a function of time and mass of carbamazepine measured on o-DGT binding gels as a function of Δg; **Figure S4**. Sketch of the floating device used for the

mesocosm experiment; **Table S1.** Sampling devices specifications; **Table S2.** Physicochemical parameters of the exposure media; **Table S3.** Limits of quantification (LOQ) for the different sampling methods; **Table S4.** Estimations of the linear uptake range; **Table S5.** Estimations of the time to equilibrium.

■ REFERENCES

Ahrens, L., Daneshvar, A., Lau, A.E., Kreuger, J., 2018. Concentrations, fluxes and field calibration of passive water samplers for pesticides and hazard-based risk assessment. Sci. Total Environ. 637–638, 835–843. https://doi.org/10.1016/j.scitotenv.2018.05.039

Amato, E.D., Covaci, A., Town, R.M., Hereijgers, J., Bellekens, B., Giacometti, V., Breugelmans, T., Weyn, M., Dardenne, F., Bervoets, L., Blust, R., 2018. A novel active-passive sampling approach for measuring time-averaged concentrations of pollutants in water. Chemosphere 209, 363–372. https://doi.org/10.1016/j.chemosphere.2018.06.079

Amato, E.D., Nguyen, D.T., Subotic, D., Hereijgers, J., Breugelmans, T., Weyn, M., Dardenne, F., Bervoets, L., Covaci, A., Town, R.M., Blust, R., 2019. Characterization of the accumulation of metals and organic contaminants on a novel active-passive sampling device under controlled water flow conditions. Chemosphere 236, 124400. https://doi.org/10.1016/j.chemosphere.2019.124400

Booij, K., Robinson, C.D., Burgess, R.M., Mayer, P., Roberts, C.A., Ahrens, L., Allan, I.J., Brant, J., Jones, L., Kraus, U.R., Larsen, M.M., Lepom, P., Petersen, J., Pröfrock, D., Roose, P., Schäfer, S., Smedes, F., Tixier, C., Vorkamp, K., Whitehouse, P., 2016. Passive Sampling in Regulatory Chemical Monitoring of Nonpolar Organic Compounds in the Aquatic Environment. Environ. Sci. Technol. 50, 3–17. https://doi.org/10.1021/acs.est.5b04050

528 Booij, K., Smedes, F., 2010. An Improved Method for Estimating in Situ Sampling Rates of
529 Nonpolar Passive Samplers. Environ. Sci. Technol. 44, 6789–6794.
530 https://doi.org/10.1021/es101321v
531 Buzier, R., Guibal, R., Lissalde, S., Guibaud, G., 2019. Limitation of flow effect on passive
532 sampling accuracy using POCIS with the PRC approach or o-DGT: A pilot-scale
533 evaluation for pharmaceutical compounds. Chemosphere 222, 628–636.
534 https://doi.org/10.1016/j.chemosphere.2019.01.181
535 Challis, J.K., Hanson, M.L., Wong, C.S., 2016. Development and Calibration of an Organic-
536 Diffusive Gradients in Thin Films Aquatic Passive Sampler for a Diverse Suite of Polar
537 Organic Contaminants. Anal. Chem. 88, 10583–10591.
538 https://doi.org/10.1021/acs.analchem.6b02749
539 Challis, J.K., Stroski, K.M., Luong, K.H., Hanson, M.L., Wong, C.S., 2018. Field Evaluation
540 and in Situ Stress Testing of the Organic-Diffusive Gradients in Thin-Films Passive
541 Sampler. Environ. Sci. Technol. 52, 12573–12582.
542 https://doi.org/10.1021/acs.est.8b03622
543 Chen, C.-E., Zhang, H., Ying, G.-G., Jones, K.C., 2013. Evidence and Recommendations to
544 Support the Use of a Novel Passive Water Sampler to Quantify Antibiotics in
545 Wastewaters. Environ. Sci. Technol. 47, 13587–13593.
546 https://doi.org/10.1021/es402662g
547 Chen, W., Li, Y., Chen, C.-E., Sweetman, A.J., Zhang, H., Jones, K.C., 2017. DGT Passive
548 Sampling for Quantitative in Situ Measurements of Compounds from Household and
549 Personal Care Products in Waters. Environ. Sci. Technol. 51, 13274–13281.
550 https://doi.org/10.1021/acs.est.7b03940
551 Davison, W., Zhang, H., 2012. Progress in understanding the use of diffusive gradients in thin
552 films (DGT)–back to basics. Environ. Chem. 9, 1–13.

553 Estoppey, N., Mathieu, J., Gascon Diez, E., Sapin, E., Delémont, O., Esseiva, P., de Alencastro,
554 L.F., Coudret, S., Folly, P., 2019. Monitoring of explosive residues in lake-bottom
555 water using Polar Organic Chemical Integrative Sampler (POCIS) and chemcatcher:
556 determination of transfer kinetics through Polyethersulfone (PES) membrane is crucial.
557 Environ. Pollut. 252, 767–776. https://doi.org/10.1016/j.envpol.2019.04.087
558 Estoppey, N., Schopfer, A., Fong, C., Delémont, O., De Alencastro, L.F., Esseiva, P., 2016.
559 An in-situ assessment of low-density polyethylene and silicone rubber passive samplers
560 using methods with and without performance reference compounds in the context of
561 investigation of polychlorinated biphenyl sources in rivers. Sci. Total Environ. 572,
562 794–803. https://doi.org/10.1016/j.scitotenv.2016.07.092
563 Estoppey, N., Schopfer, A., Omlin, J., Esseiva, P., Vermeirssen, E.L.M., Delémont, O., De
564 Alencastro, L.F., 2014. Effect of water velocity on the uptake of polychlorinated
565 biphenyls (PCBs) by silicone rubber (SR) and low-density polyethylene (LDPE)
566 passive samplers: An assessment of the efficiency of performance reference
567 compounds (PRCs) in river-like flow conditions. Sci. Total Environ. 499, 319–326.
568 https://doi.org/10.1016/j.scitotenv.2014.08.047
569 Gaulier, C., Zhou, C., Guo, W., Bratkic, A., Superville, P.-J., Billon, G., Baeyens, W., Gao,
570 Y., 2019. Trace metal speciation in North Sea coastal waters. Sci. Total Environ. 692,
571 701–712. https://doi.org/10.1016/j.scitotenv.2019.07.314
572 Guo, W., Van Langenhove, K., Vandermarken, T., Denison, M.S., Elskens, M., Baeyens, W.,
573 Gao, Y., 2019. In situ measurement of estrogenic activity in various aquatic systems
574 using organic diffusive gradients in thin-film coupled with ERE-CALUX bioassay.
575 Environ. Int. 127, 13–20. https://doi.org/10.1016/j.envint.2019.03.027

576 Harman, C., Allan, I.J., Bäuerlein, P.S., 2011. The Challenge of Exposure Correction for Polar
577 Passive Samplers—The PRC and the POCIS. Environ. Sci. Technol. 45, 9120–9121.
578 https://doi.org/10.1021/es2033789
579 Harman, C., Allan, I.J., Vermeirssen, E.L.M., 2012. Calibration and use of the polar organic
580 chemical integrative sampler—a critical review. Environ. Toxicol. Chem. 31, 2724–
581 2738. https://doi.org/10.1002/etc.2011
582 Harman, C., Booij, K., 2014. Letter to the Editor Concerning the Viewpoint; "Recognizing the
583 Limitations of Performance Reference Compound (PRC)-Calibration Technique in
584 Passive Water Sampling." Environ. Sci. Technol. 48, 3–3.
585 https://doi.org/10.1021/es405153c
586
587 Huckins, J. N.; Petty, J. D.; Lebo, J. A.; Almeida, F. V.; Booij, K.; Alvarez, D. A.; Cranor, W.
588 L.; Clark, R. C.; Mogensen, B. B. Development of the permeability/performance
589 reference compound approach for in situ calibration of semipermeable membrane
590 devices. Environ. Sci. Technol. 2002, 36, 85–91. https://doi.org/10.1021/es010991w
591
592 Jonker, M.T.O., Muijs, B., 2010. Using solid phase micro extraction to determine salting-out
593 (Setschenow) constants for hydrophobic organic chemicals. Chemosphere 80, 223–
594 227. https://doi.org/10.1016/j.chemosphere.2010.04.041
595 Kaserzon, S.L., Kennedy, K., Hawker, D.W., Thompson, J., Carter, S., Roach, A.C., Booij, K.,
596 Mueller, J.F., 2012. Development and Calibration of a Passive Sampler for
597 Perfluorinated Alkyl Carboxylates and Sulfonates in Water. Environ. Sci. Technol. 46,
598 4985–4993. https://doi.org/10.1021/es300593a

599 Li, Y.-H., Gregory, S., 1974. Diffusion of ions in sea water and in deep-sea sediments.
600 Geochim. Cosmochim. Acta 38, 703–714. https://doi.org/10.1016/0016-
601 7037(74)90145-8
602 Liu, H.-H., Wong, C.S., Zeng, E.Y., 2013. Recognizing the Limitations of Performance
603 Reference Compound (PRC)-Calibration Technique in Passive Water Sampling.
604 Environ. Sci. Technol. 47, 10104–10105. https://doi.org/10.1021/es403353d
605 Lohmann, R., Muir, D., Zeng, E.Y., Bao, L.-J., Allan, I.J., Arinaitwe, K., Booij, K., Helm, P.,
606 Kaserzon, S., Mueller, J.F., Shibata, Y., Smedes, F., Tsapakis, M., Wong, C.S., You,
607 J., 2017. Aquatic Global Passive Sampling (AQUA-GAPS) Revisited: First Steps
608 toward a Network of Networks for Monitoring Organic Contaminants in the Aquatic
609 Environment. Environ. Sci. Technol. 51, 1060–1067.
610 https://doi.org/10.1021/acs.est.6b05159
611 Macoustra, G., Holland, A., Stauber, J., Jolley, D.F., 2019. Effect of Various Natural Dissolved
612 Organic Carbon on Copper Lability and Toxicity to the Tropical Freshwater Microalga
613 Chlorella sp. Environ. Sci. Technol. 53, 2768–2777.
614 https://doi.org/10.1021/acs.est.8b04737
615 Mazzella, N., Lissalde, S., Moreira, S., Delmas, F., Mazellier, P., Huckins, J.N., 2010.
616 Evaluation of the Use of Performance Reference Compounds in an Oasis-HLB
617 Adsorbent Based Passive Sampler for Improving Water Concentration Estimates of
618 Polar Herbicides in Freshwater. Environ. Sci. Technol. 44, 1713–1719.
619 https://doi.org/10.1021/es902256m
620 Morin, N., Miège, C., Coquery, M., Randon, J., 2012. Chemical calibration, performance,
621 validation and applications of the polar organic chemical integrative sampler (POCIS)
622 in aquatic environments. TrAC Trends Anal. Chem., Chemical Monitoring Activity for

623 the Implementation of the Water Framework Directive 36, 144–175.
624 https://doi.org/10.1016/j.trac.2012.01.007
625 Poulier, G., Lissalde, S., Charriau, A., Buzier, R., Delmas, F., Gery, K., Moreira, A., Guibaud,
626 G., Mazzella, N., 2014. Can POCIS be used in Water Framework Directive
627 (2000/60/EC) monitoring networks? A study focusing on pesticides in a French
628 agricultural watershed. Sci. Total Environ. 497, 282–292.
629 Rusina, T.P., Smedes, F., Koblizkova, M., Klanova, J., 2010. Calibration of Silicone Rubber
630 Passive Samplers: Experimental and Modeled Relations between Sampling Rate and
631 Compound Properties. Environ. Sci. Technol. 44, 362–367.
632 https://doi.org/10.1021/es900938r
633 Scally, S., Davison, W., Zhang, H., 2006. Diffusion coefficients of metals and metal complexes
634 in hydrogels used in diffusive gradients in thin films. Anal. Chim. Acta 558, 222–229.
635 https://doi.org/10.1016/j.aca.2005.11.020
636 Smedes, F., 2019. SSP silicone–, lipid– and SPMD–water partition coefficients of seventy
637 hydrophobic organic contaminants and evaluation of the water concentration calculator
638 for SPMD. Chemosphere 223, 748–757.
639 https://doi.org/10.1016/j.chemosphere.2019.01.164
640 Smedes, F., Booij, K., 2012. Guidelines for passive sampling of hydrophobic contaminants in
641 water using silicone rubber samplers. International Council for the Exploration of the
642 Sea.
643 Strivens, J., Hayman, N., Rosen, G., Myers- Pigg, A., 2020. Toward Validation of
644 Toxicological Interpretation of Diffusive Gradients in Thin Films in Marine Waters
645 Impacted by Copper. Environ. Toxicol. Chem. 39, 873–881.
646 https://doi.org/10.1002/etc.4673

Stroski, K.M., Challis, J.K., Wong, C.S., 2018. The influence of pH on sampler uptake for an improved configuration of the organic-diffusive gradients in thin films passive sampler. Anal. Chim. Acta 1018, 45–53. https://doi.org/10.1016/j.aca.2018.02.074

Tomaszewski, L., Buffle, J., Galceran, J., 2003. Theoretical and Analytical Characterization of a Flow-Through Permeation Liquid Membrane with Controlled Flux for Metal Speciation Measurements. Anal. Chem. 75, 893–900. https://doi.org/10.1021/ac020486x

Uher, E., Tusseau-Vuillemin, M.-H., Gourlay-France, C., 2013. DGT measurement in low flow conditions: diffusive boundary layer and lability considerations. Environ. Sci. Process. Impacts 15, 1351–1358. https://doi.org/10.1039/C3EM00151B

van der Veeken, P.L., Chakraborty, P. and van Leeuwen, H.P., 2010. Accumulation of humic acid in DET/DGT gels. Environ. Sci. Technol. 44, 4253-4257. https://doi.org/10.1021/es100510u

van der Veeken, P.L. and van Leeuwen, H.P., 2010. DGT/DET gel partition features of humic acid/metal species. Environ. Sci. Technol. 44, 5523-5527. https://doi.org/10.1021/es100861t

van Leeuwen, H.P., Town, R.M., Buffle, J., Cleven, R.F.M.J., Davison, W., Puy, J., van Riemsdijk, W.H., Sigg, L., 2005. Dynamic Speciation Analysis and Bioavailability of Metals in Aquatic Systems. Environ. Sci. Technol. 39, 8545–8556. https://doi.org/10.1021/es050404x

van Leeuwen, H. P. 2016. Revisited: DGT speciation analysis of metal-humic acid complexes. Environ. Chem. 13, 84-88. https://doi.org/10.1071/EN15066

Warnken, K.W., Zhang, H., Davison, W., 2006. Accuracy of the diffusive gradients in thin-films technique: diffusive boundary layer and effective sampling area considerations. Anal. Chem. 78, 3780–3787.

Yezek, L., van Leeuwen, H. P. 2005. Donnan effects in the steady-state diffusion of metal ions through charged thin films. Langmuir, 21, 10342-10347. https://doi.org/10.1021/la050159v

Yezek, L., van der Veeken, P. L. R., van Leeuwen, H. P. 2008. Donnan effects in metal speciation analysis by DET/DGT. Environ. Sci. Technol. 42, 9250-9254. https://doi.org/10.1021/es8021232